

---

# Versatile Multimodal Controls for Whole-Body Talking Human Animation

---

Zheng Qin<sup>1</sup> Ruobing Zheng<sup>†2</sup> Yabing Wang<sup>1</sup> Tianqi Li<sup>2</sup> Zixin Zhu<sup>3</sup> Minghui Yang<sup>2</sup> Ming Yang<sup>2</sup>  
Le Wang<sup>\*1</sup>

## Abstract

Human animation from a single reference image shall be flexible to synthesize whole-body motion for either a headshot or whole-body portrait, where the motions are readily controlled by audio signal and text prompts. This is hard for most existing methods as they only support producing pre-specified head or half-body motion aligned with audio inputs. In this paper, we propose a versatile human animation method, *i.e.*, **VersaAnimator**, which generates whole-body talking human from arbitrary portrait images, not only driven by audio signal but also flexibly controlled by text prompts. Specifically, we design a text-controlled, audio-driven motion generator that produces whole-body motion representations in 3D synchronized with audio inputs while following textual motion descriptions. To promote natural smooth motion, we propose a code-pose translation module to link VAE codebooks with 2D DWposes extracted from template videos. Moreover, we introduce a multi-modal video diffusion that generates photo-realistic human animation from a reference image according to both audio inputs and whole-body motion representations. Extensive experiments show that VersaAnimator outperforms existing methods in visual quality, identity preservation, and audio-lip synchronization.

## 1. Introduction

Talking human video generation aims to animate a portrait (or an avatar) from control signals such as audio, text and pose sequences, producing realistic and natural talking human. This has emerged as a prominent and rapidly growing research direction within video generation, with a wide range of applications in education (Seeger et al., 2021), healthcare (Seitz et al., 2022) and live streaming (Li et al., 2021a), *etc.*

<sup>†</sup>Project lead, <sup>\*</sup>Corresponding author, <sup>1</sup>Xi'an Jiaotong University, <sup>2</sup>Ant Group, <sup>3</sup>University at Buffalo.

Existing works start from synthesizing talking head for audio-driven speaker video generation (Tian et al., 2025; Wang et al., 2024a; Xu et al., 2024b), where the focuses of human motion generation are primarily on the lip and facial expressions within the head-shoulder region. To enhance the expressiveness of a speaker, later efforts (Corona et al.; Lin et al., 2024; Meng et al., 2024) extend the animation generation to include the upper body, enabling natural and gestural movements.

These methods can well handle some formal scenarios, such as news broadcasting or speeches, where the generated body motions are typically restricted to the gestures of a reference figure, only involving the upper body without the lower body. Actually, this is quite restrictive, as in talk shows or crosstalk performances, whole-body human motion is essential to impress audiences with infectious speech. Besides, since persons seldom hold still during speaking, whole-body motion shall be generated even for a half-body reference image. Nevertheless, how can we generate whole-body motion for an arbitrary reference 1/4, 1/2 headshot or a whole body portrait, truly extending a talking head to talking human?

The whole-body motion of an audio-driven talking human needs to synchronize with the given audio control signal. Though audio signal can precisely determine lip motion, it is hard to associate audio with specific body motion, since there are multiple ways to convey the same message by body language in different cultures or by different persons. Therefore, this inherent diversity requires users to specify body motion in a speech. In prior work, users have no control over the character's action, *e.g.*, requiring him to wave goodbye with the left hand or right hand to audiences around the closing words in Figure 1. Thus, how can we allow users to use convenient text prompts to control or edit the body motion generation flexibly?

In this paper, we would like to generate a whole-body talking human from a single reference figure image, either a headshot or portrait, and allow users to employ multimodality controls, *i.e.*, audio signal plus text prompts, to flexibly control or edit the body motion generation. Therefore, we propose a versatile audio-driven talking human generation method, abbreviated as VersaAnimator. This animator consists of two key components: a motion generator that pro-

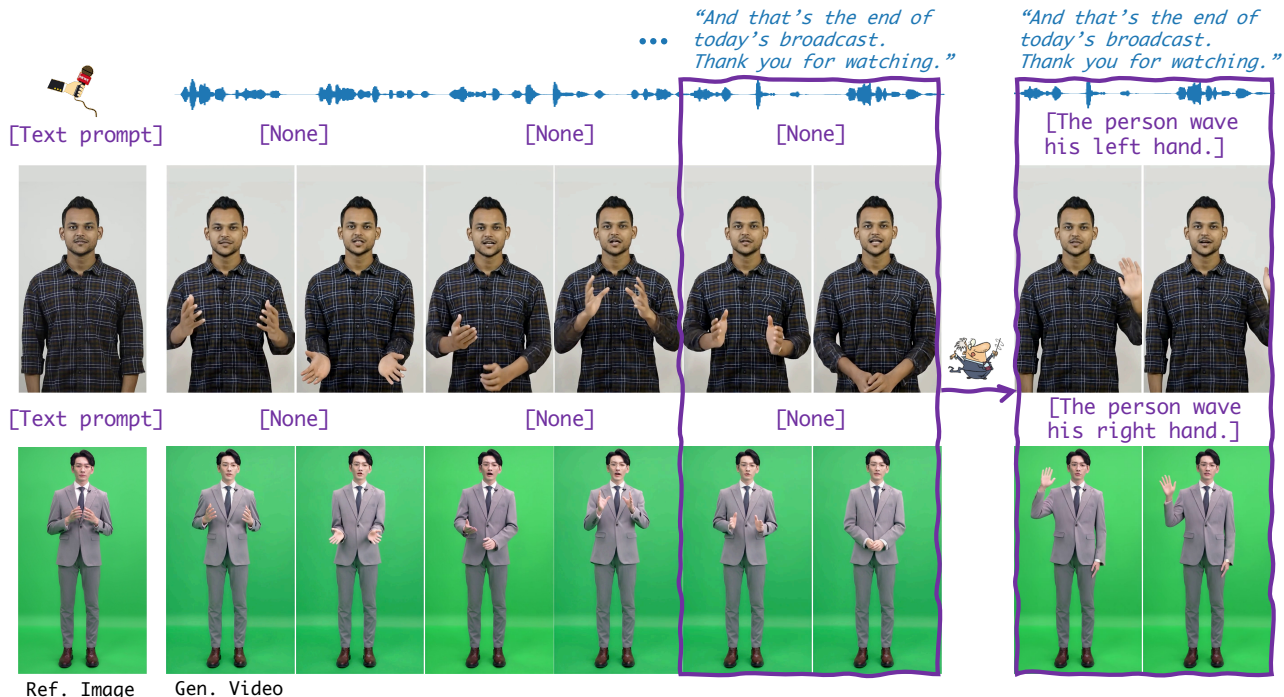


Figure 1. Given a reference image in the first column and an audio clip, our method generates photorealistic talking videos of the person. As demonstrated in the synthesized images, our approach supports arbitrary reference images, *i.e.*, semi-body in the upper demo and whole-body in the lower, and allows users to control or edit the body motion by text prompts, *e.g.* waving different hands at the closing.

duces pose sequences synchronized with the given audio signal while following the text prompts of body motion; and a multimodal diffusion module that generates talking human video based on the reference image, no matter a 1/4, 1/2 or full-body portrait. We argue that if the input reference only involves upper body, the generation of the whole-body motion still contributes to natural head or upper-body movements during speaking, even only the upper-body regions are rendered as required by users.

Specifically, VersaAnimator generates human pose sequences in 3D first and maps them back to 2D pose sequences later, since 3D human motion offers precise control over the movement of bones and joints. Besides, 3D motion datasets (Guo et al., 2022a) are readily accessible to learn the text-to-motion semantic association. Afterwards, we construct a set of motion tokens to unify the motion representation across different datasets by training a VQ-AVE. To support the multimodal control, we design a two-branch transformer that generates motions conditioned on both audio and text prompts. We further design a new code-pose translation module to synthesize natural and smooth motion when mapping 3D motions to 2D pose sequences, by constructing a relation bank that links the VQ-VAE codebook to 2D poses. Finally, we employ a multimodal diffusion model that incorporate both audio control signal and the 2D pose sequence to produce a talking human aligned with the audio

lip sync and expressions. This diffusion model is trained in two stages, learning the whole-body movement first and then the audio-driven facial movement generation.

We have constructed a 40-hour human animation training set that spans from head to whole-body human videos, collected from the internet. Extensive qualitative and quantitative experiments demonstrate that our method achieves state-of-the-art performance in terms of both robustness and naturalness across a wide range of reference images. In addition, our VersaAnimator exhibits excellent text-controlled motion generation capability on the HumanML3D benchmark (Guo et al., 2022a). To our best knowledge, this is the first work dedicated to generating whole-body talking human, with the following contributions:

- We propose to generate whole-body motions for arbitrary reference images, with no restriction on the visible body region in the reference. The generation of lower body movements enhances the expressiveness of a talking human, even only half-body videos are rendered if required by users, by presenting subtle sway in sync with natural talking rhythm.
- We design a text-controlled, audio-driven motion generator that produces pose sequences synchronized with the given audio signal, while allowing users to flexibly

control or edit body motion generation using convenient text prompts.

- We design a multimodal diffusion model with two-stage training process for human video generation, learning the whole-body movement first and then the audio-driven facial movement generation.

## 2. Related work

**Human Video Generation.** In terms of the target region, existing works have focused on either head or body. Remarkable efforts (Tian et al., 2025; Wang et al., 2024a; Xu et al., 2024b; Chen et al., 2024; Zhang et al., 2023c; Ma et al., 2023; Wang et al., 2021; Yin et al., 2022; Prajwal et al., 2020) have concentrated on audio-driven speaker video generation, primarily focusing on the head-shoulder region especially facial expressions, in speech-driven scenarios. Recent efforts (Zhang et al., 2024b; Zhu et al., 2025; Wang et al., 2024b; Feng et al., 2023; Xu et al., 2024c; Hu, 2024; Chang et al., 2023; Karras et al., 2023; Ma et al., 2024) have focused on driving character animation through pose guidance. To enhance expressiveness and realism, VLOGGER (Corona et al.) and CyberHost (Lin et al., 2024) generate half-body talking videos with movements using only audio and reference maps as inputs. EchoMimicV2 (Meng et al., 2024) need for gesture movements as input in addition to audio. Despite recent advancements, they still exhibit several limitations, such as quite limited body motion and a lack of fine-grained control of gesture movements in the generated videos.

**Human Motion Generation.** Human motion generation can be broadly categorized into two primary approaches *w.r.t.* the control inputs: 1) motion synthesis without conditions (Raab et al., 2022; Tevet et al., 2022; Zhang et al., 2020) and 2) motion synthesis with specified multimodal conditions, such as action labels (Xu et al., 2022; Lee et al., 2022; Dou et al., 2023), textual descriptions (Wang et al.; Chen et al., 2022; Lu et al., 2023), or audio and music (Li et al., b; Tseng et al., 2022; Li et al., a; Dabral et al., 2022). Due to its user-friendly nature and the convenience of language input, text-to-motion is one of the most important motion generation tasks. Given the remarkable success of diffusion-based generative models on AIGC tasks (Rombach et al., 2022), some approaches have employed conditional diffusion models for human motion generation (Zhang et al., 2024a; Chen et al., 2023). Other works (Zhang et al., 2023a; Guo et al., 2024; Wang, 2023) first discretize motions into tokens using vector quantization (Van Den Oord et al., 2017) and then predict the code sequence of motion.

## 3. Method

### 3.1. Preliminary and Overview

**3D Human Motion Representation.** SMPL (Skinned Multi-Person Linear Model) (Loper et al., 2023) is a widely used method for modeling human shape and posture, representing the 3D geometry of the human body through Linear Blend Skinning. It allows the body to adapt a variety of poses that are controlled and rationalized by a set of joint parameters, denoted as  $j \in \mathbb{R}^{3J}$ , where  $J$  is the number of joints and the factor of 3 corresponds to the  $x, y, z$  coordinates in 3D space, representing the positional parameters of each joint. A sequence of poses can express a continuous motion, represented as  $\{j_t\}_{t=1}^T$ . In particular, the 6D continuous rotation representation from (Zhou et al., 2019) is developed to generate a compact yet comprehensive representation  $\{m_t\}_{t=1}^T$ , where  $m_t$  represents the motion representation at frame  $t$ , encompassing crucial details such as positional rotation and velocity. This approach proves advantageous for accurately modeling human motion.

3D human motions are highly controllable with a rich dataset available (Guo et al., 2022a), containing a variety of motion data paired with corresponding textual descriptions. This motivates us to utilize 3D motions as the whole-body motion representation. On one hand, this enhances the authenticity and plausibility of human motions in videos. On the other hand, by leveraging the rich text-3D motion correspondence data, we can enable users to use convenient text prompts to control or edit the body motion generation flexibly in generated video.

**Overview of VersaAnimator.** Given an audio input and text prompts, our VersaAnimator can animate the reference character to synchronize with the speech while also following the textual prompt of body motions. The audio is divided into multiple clips for generating talking videos, and the text prompt controls the motion of the corresponding clip based on the user’s specifications. As shown in Figure 2, the inference process consists of three stages: (a) The Motion Generator (Section 3.2) takes both audio and text prompts as inputs, generating human motion in 3D conditioned on them, which is then input into the Motion Translator (Section 3.2.4) to synthesize a 2D pose sequence. (b) After that, we construct the pose and audio conditions to be used in the next stage (Section 3.3). (c) We inject both conditions into the diffusion model to animate the reference character for video generation (Section 3.3).

### 3.2. Audio-driven Motion Generation with Text Control

In this section, we first discretize the motions and then focus on generating motion tokens driven by both audio and text. To enable motion generation conditioned on multiple modalities, *i.e.*, audio and text, we adopt a two-branch

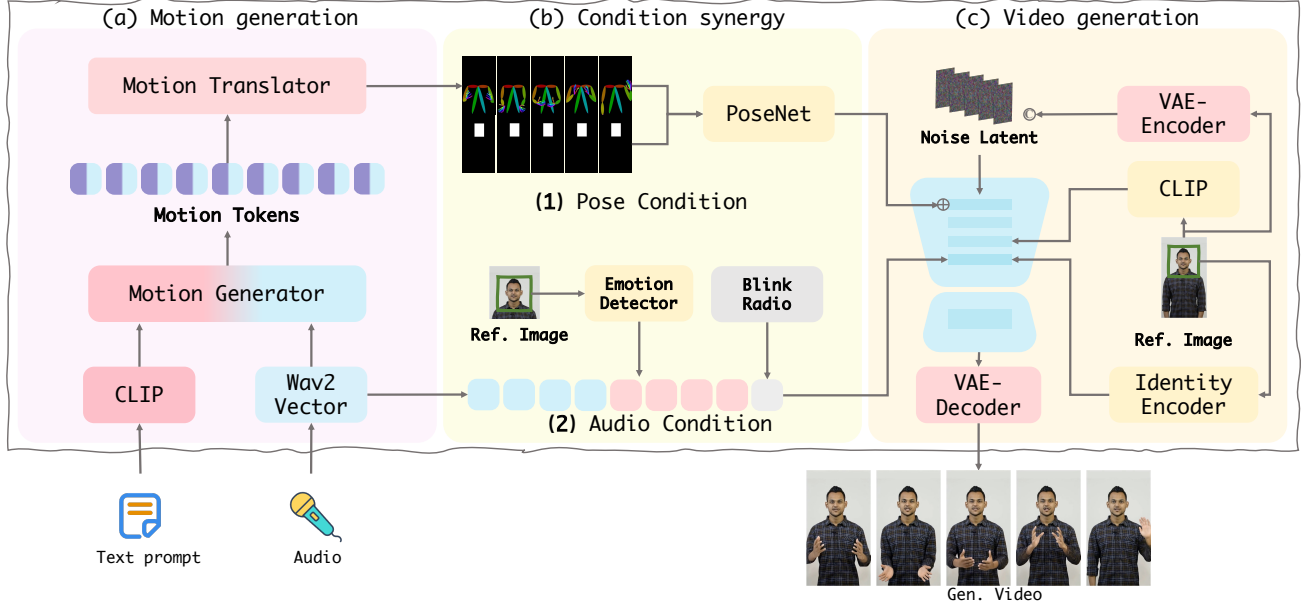


Figure 2. Overview of our VersaAnimator. The **Motion Generation** process uses both audio and text modalities to specify the facial and body motion to generate. Then **Condition Synergy** process generates the pose condition and audio condition as the control signal in video generation. Finally, we inject both conditions into the diffusion model to animate the reference character for **Video Generation**.

architecture. This architecture consists of a primary audio-to-motion branch and a plug-and-play text control branch, supported by a two-stage training strategy.

### 3.2.1. 3D HUMAN MOTION TOKENIZER

Vector Quantized Variational Autoencoders (VQ-VAE) (Van Den Oord et al., 2017) enable the learning of discrete representations, offering significant advantages for content compression and generation. VQ-VAE reconstructs the motion sequence using an autoencoder with a learnable  $K$ -size codebook  $C = \{c_k\}_{k=1}^K$ , where each code  $c_k \in \mathbb{R}^{d_c}$  corresponds to a discretized feature, and  $d_c$  denotes the dimension of the discretized feature. Given a motion sequence  $M = \{m_t\}_{t=1}^T$ , the encoder  $\mathcal{E}$  maps it into a latent feature sequence  $Z = \{z_i\}_{i=1}^{T/l}$ , where  $z_i \in \mathbb{R}^{d_c}$  and  $l$  is the temporal downsampling rate of  $\mathcal{E}$ . For each latent feature  $z_i$ , quantization is performed by selecting the closest element in  $C$ , resulting in the quantized feature sequence  $\hat{Z} = \{\hat{z}_i\}_{i=1}^{T/l}$ , as follows:

$$\hat{z}_i = \arg \min_{c_k \in C} \|z_i - c_k\|_2,$$

where  $\hat{z}_i$  is the quantized version of  $z_i$ . Finally, the decoder  $\mathcal{D}$  reconstructs the motion sequence  $\hat{M}$  from the quantized feature sequence  $\hat{Z}$ . We construct a 512-size codebook, where the motion tokens are used to combine and express coherent movements of the human body.

### 3.2.2. MOTION GENERATION ARCHITECTURE

**Audio Token.** We utilize wav2vec (Schneider et al., 2019) as our audio tokenizer and we design a temporal block consists of multiple convolution layers to extract and fuse the temporal information.

We implement the transformer  $p_\theta^{audio}(z|audio)$  as the primary audio-to-motion architecture. The goal is to predict the code sequence (responded to motion tokens in codebook) conditioned by the audio signal. Specifically, the audio tokens are fed into the transformer encoder to capture long-range dependencies and contextual relationships within the audio sequence. The outputs of each transformer layer are gathered and denoted by  $\{f_s^{audio}\}_{s=1}^S$ , where  $f_s^{audio}$  represent the  $s$ -th layer’s output and  $S$  is set to 8. Then utilizing simple linear layers, we convert last feature  $f_S^{audio}$  to code probability  $I^{audio} \in \mathbb{R}^{T \times K}$ , where  $T$  and  $K$  represent the predicted motion length and size of the codebook respectively. At timestamp  $t$ , the probability distribution of the motion codes is as follows:

$$P(m_t = c_k) = p_k^t, \quad k = 1, \dots, K. \quad (1)$$

Then, we select the code sequence  $\{c_i\}_{i=1}^{T/l}$  that matches the audio signal through the probability distribution  $I^{audio}$ . Finally, a well-trained decoder and corresponding codebook convert the code sequence into the motion  $M = \{m_t\}_{t=1}^T$ .

**Multimodal Conditions** To edit the motion of animated character with text, *i.e.*, to allow the text to control the



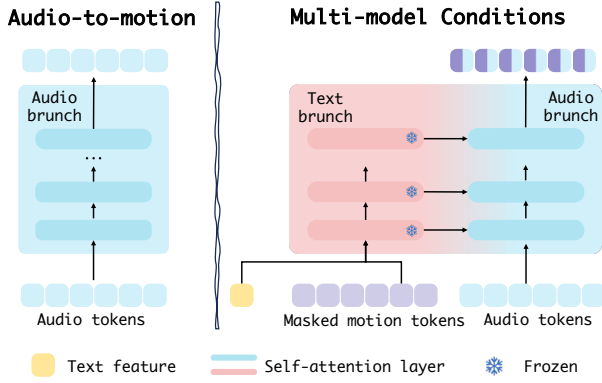


Figure 3. Structure of the motion generator. Left: The primary audio-to-motion architecture. Right: The two-branch transformer that generates motions conditioned on both audio and text prompts.

prediction of the motion token, we add an extra text control branch  $p_{\theta}^{text}(z|text)$ . Specifically, we learn a text-to-motion transformer to model the tokens conditioned on text. The text-to-motion transformer has the same architecture as the primary audio-to-motion model. Given the text signal, we use CLIP (Radford et al., 2021) for extracting text features and feed into text-to-motion transformer and obtain  $\{f_s^{text}\}_{s=1}^S$ , where  $f_s^{text}$  represents the  $s$ -th layer’s output. We then consolidate  $p_{\theta}^{audio}(z|audio)$  and  $p_{\theta}^{text}(z|text)$  by summing them layer by layer.

### 3.2.3. TRAINING

**Training 3D Human Motion Tokenizer.** Overall, the VQ-VAE is trained via a motion reconstruction loss combined with a latent embedding loss at quantization layer:

$$\mathcal{L}_{mdr} = \|M - \hat{M}\|_1 + \beta \left\| Z - \text{sg} \left[ \hat{Z} \right] \right\|_2^2, \quad (2)$$

where  $\text{sg}[\cdot]$  denotes the stop-gradient operation, and  $\beta$  a weighting factor for embedding constraint. The codebooks are updated via exponential moving average and codebook reset following (Zhang et al., 2023a).

**Training Motion Generation Model.** We first train the text to motion branch, then freeze the weights and train the audio to motion branch. For text to motion branch, we randomly mask out the sequence elements, by replacing the tokens with a special mask token. The goal is to predict the masked tokens given text. We use CLIP (Radford et al., 2021) for extracting text features. Our training goal is to predict the masked tokens. We directly maximize the log-likelihood of the data distribution  $p(\hat{M} | text)$ :

$$\mathcal{L}_{\text{tran}} = \mathbb{E}_{\hat{M} \sim p(\hat{M})} [-\log p(\hat{M} | text)], \quad (3)$$

the likelihood of the full sequence is denoted as follows:

$$p(\hat{M} | text) = \prod_{i=1}^{T/l} (p(\hat{m}_t | text) \cdot (1 - [mask]_t) + [mask]_t), \quad (4)$$

where  $[mask]_t$  indicates whether the  $i$ -th token is masked, which is set to 0 if masked, and 1 otherwise.

During training the audio-to-motion branch, we set the text “A person is giving a speech.” as text control. Given the input text control and audio tokens, the training objective is:

$$\mathcal{L}_{\text{res}} = \sum_{i=1}^n -\log p_{\phi}(m_i | a_i, text), \quad (5)$$

where  $m_i$  and  $a_i$  are the  $i$ -th motion and audio token respectively.

### 3.2.4. CODE-POSE TRANSLATION CONSTRUCTION

After obtaining the code sequence (motion tokens), the next step is to map them to 2D pose sequences for video generation. Directly mapping 3D human model to 2D pose often results in stiff and unrealistic motions. To address this issue, we construct a relation bank that links the VQ-VAE codebook to 2D poses. Specifically, we extract the SMPL-X data (Cai et al., 2024) and 2D dwpose (Yang et al., 2023) of the template videos, and use the previously trained 3D human motion tokenizer to convert them into code sequences. This allows us to establish the correspondence between the code and 2d pose. By extracting real-world poses from template videos and aligning them with the codes in the codebook, we can create a large set of code-2D pose pairs, thereby enhancing the realism of the generated motions.

## 3.3. Generating Photorealistic Talking and Moving Humans with Audio and Motion Control

We aim to generate videos with accurate lip synchronization and rich gestures from a single image and audio input. Since there is only indirect weak correlation between audio and body movements, generating whole-body movements solely based on audio input remains challenging. Therefore, we pre-generate motion representations using the aforementioned Motion Generation module, then transform these motion representations into explicit pose sequences, combined with audio and a single reference image to produce the final video. To accomplish this task, we first construct a multimodal-controlled video diffusion model.

### 3.3.1. CO-SPEECH HUMAN ANIMATION WITH VIDEO DIFFUSION MODEL

We extend an off-the-shelf human animation framework (Zhang et al., 2024b) by incorporating additional conditional signal, including audio, emotion labels, and

blinking ratios. This enhancement enables the simultaneous generation of lip movements and whole-body animations.

As shown in Figure 2, we refine the original whole-body pose sequence extracted from video frames (Hu, 2024) into a composite representation, which combines the body pose below the neck with a fixed-size head mask centered on the facial midpoint above the neck. This design circumvents the impact of facial keypoints in original pose sequences on generating synthesized facial movements, thereby enabling lip movements and facial expressions in generated videos to be driven by subsequent audio inputs and other control signals. This composite representation is then mapped through PoseNet and element-wise added to the output of the U-Net’s first convolution layer (Zhang et al., 2024b). In addition, along with extracting image features from the reference image, we detect the facial region and extract an identity embedding using a pre-trained face recognition network (Deng et al., 2018). We draw inspiration from the Cyberhost (Lin et al., 2024) and introduce an additional cross-attention layer after the original cross-attention layer in every U-Net block, specifically designed to generate facial dynamics. Notably, we adopt the strategy from (Li et al., 2024) to incorporate conditional signal directly related to facial motion, including audio, expression labels, and blink ratio, as an additional control signal that interacts with the identity embedding in the new cross-attention layer. This design mitigates the ambiguity inherent in purely audio-driven approaches, leading to accurate generation of lip motions, facial expressions, and eye blinking while maintaining strong identity consistency.

### 3.3.2. TRAINING STRATEGY

We employ a two-stage training strategy to train the rendering module. Given that the original pose-guided SVD backbone (Zhang et al., 2024b) is typically trained on whole-body dance data, we first fine-tune it using collected close-up human talking videos to enhance the generation of magnified facial details. Subsequently, we introduce additional control signals and train the complete network controlled by both audio and pose. In the second stage, we utilize human talking videos with audio-visual synchronization at various scales, including whole-body standing postures, close-up seated postures, and the talking-head scale. For each training videos, we extract audio features as (Xu et al., 2024a) and randomly select one frame as a reference image to extract image features and identity features (Lin et al., 2024).

## 4. Experiments

### 4.1. Setting

**Training Data and Evaluation Benchmark Construction.** To train the multimodal diffusion model, we collect about 40

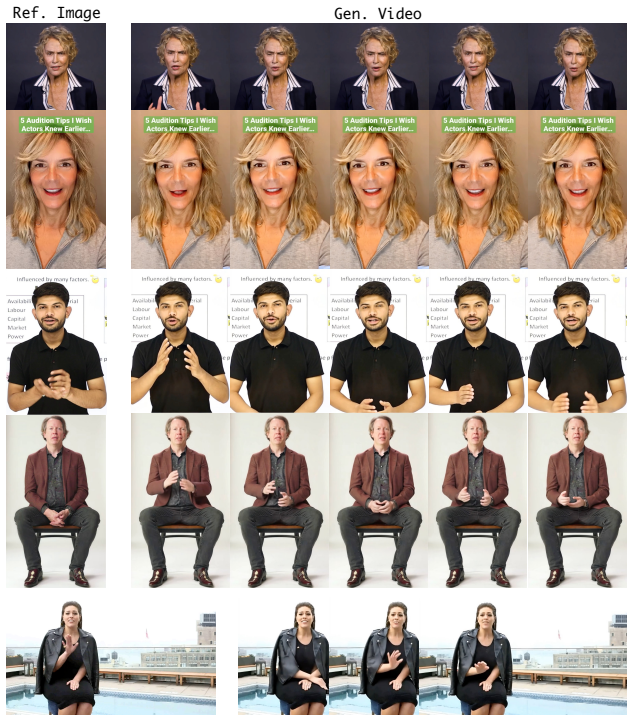


Figure 4. Results on Multi-Animate with different audio and reference images (ranging from head to whole-body).

hours of human talking videos with a variety of visible body regions, from head to whole body, including multiple nationalities, languages, and ages. We sample from the above videos to create an audio-to-motion dataset and combine it with the HumanML3D (Guo et al., 2022a) dataset to train a text-controlled, audio-driven motion generator.

Publicly available datasets typically focus on evaluating audio-driven talking head or pose-driven character animations, while whole-body talking videos are scarce in existing datasets. To evaluate human animation comprehensively from multiple perspectives such as facial generation, motion generation, and rendering quality, we introduce a multi-scale human animation evaluation benchmark, named Multi-Animate. This benchmark features human talking videos ranging from head-only to whole-body animations. Our dataset includes 30 human talking videos with 100 speech segments, covering various body scales, nationalities, and languages.

**Metrics.** We evaluate the performance of text-to-motion generation using R-Precision (Guo et al.) and Frechet Inception Distance (FID) (Heusel et al., 2017), which reflect semantic consistency and the overall motion quality, respectively. For human video generation, we employ a range of metrics. FID, FVD (Unterthiner et al., 2018), SSIM (Wang et al., 2004), and PSNR (Hore & Ziou, 2010) are used to assess low-level visual quality, while E-

Table 1. Quantitative comparison and ablation study of our proposed VersaAnimator on multi-scale animation benchmark, *Multi-Animate*.

| METHODS                           | FID↓         | FVD↓          | SSIM↑       | PSNR↑        | E-FID↓      | SYNC-D↓     | SYNC-C↑     | CSIM↑       |
|-----------------------------------|--------------|---------------|-------------|--------------|-------------|-------------|-------------|-------------|
| MIMICMOTION (ZHANG ET AL., 2024B) | 39.25        | 220.69        | 0.13        | 16.64        | <b>1.90</b> | 9.97        | 4.96        | 0.65        |
| ECHOMIMICV2 (MENG ET AL., 2024)   | 38.40        | 443.48        | 0.19        | 15.51        | 2.92        | 9.46        | 5.34        | 0.63        |
| VERSAANIMATOR                     | <b>16.28</b> | <b>128.40</b> | <b>0.26</b> | <b>20.69</b> | 3.12        | <b>8.85</b> | <b>6.55</b> | <b>0.99</b> |
| VERSAANIMATOR*                    | 29.28        | 235.84        | 0.32        | 16.44        | 7.73        | 8.57        | 6.75        | 0.74        |
| W/O CODE TRANSLATE                | 32.34        | 302.87        | 0.23        | 14.31        | 8.42        | 8.23        | 6.91        | 0.73        |
| W/O PER-LAYER FUSION              | 30.14        | 240.56        | 0.30        | 16.12        | 7.23        | 8.59        | 6.64        | 0.79        |
| W/O TEXT BRANCH                   | 29.12        | 220.67        | 0.34        | 17.02        | 7.45        | 8.34        | 6.78        | 0.71        |

Table 2. Evaluation of text-to-motion capability on the HumanML3D test set, with comparison to state-of-the-art methods such as TM2T (Guo et al., 2022b), T2M (Guo et al.), MDM (Shafir et al., 2023), MLD (Chen et al., 2023), MotionDiffuse (Zhang et al., 2022b), T2M-GPT (Zhang et al., 2023a), and ReMoDiffuse (Zhang et al., 2023b).

| METHODS       | R PRECISION↑      |                   |                   | FID↓              |
|---------------|-------------------|-------------------|-------------------|-------------------|
|               | TOP 1             | TOP 2             | TOP 3             |                   |
| TM2T          | 0.424±.003        | 0.618±.003        | 0.729±.002        | 1.501±.017        |
| T2M           | 0.455±.003        | 0.636±.003        | 0.736±.002        | 1.087±.021        |
| MDM           | -                 | -                 | 0.611±.007        | 0.544±.044        |
| MLD           | 0.481±.003        | 0.673±.003        | 0.772±.002        | 0.473±.013        |
| MOTIONDIFFUSE | 0.491±.001        | 0.681±.001        | 0.782±.001        | 0.630±.001        |
| T2M-GPT       | 0.492±.003        | 0.679±.002        | 0.775±.002        | 0.141±.005        |
| REMODIFFUSE   | 0.510±.005        | 0.698±.006        | 0.795±.004        | 0.103±.004        |
| OURS          | <b>0.505±.002</b> | <b>0.698±.003</b> | <b>0.794±.002</b> | <b>0.090±.003</b> |

FID (Deng et al., 2019) is used to evaluate the authenticity of the generated images. CSIM is employed to measure identity consistency. Additionally, we use SyncNet (Prajwal et al., 2020) to calculate Sync-C and Sync-D, which validate the accuracy of audio-lip synchronization.

**Implementation Details.** We implemented our VersaAnimator in PyTorch (Paszke et al., 2019), and performed all experiments on NVIDIA A100 GPUs (80GB). The motion generation and video generation components are trained on 1 and 8 GPUs, respectively. All implementation and training details are provided in the supplementary material.

## 4.2. Quantitative Results

**Multi-scale Human Animation.** Given an audio, our method generates a talking video featuring the character from the reference image. As shown in Figure 4, we present the generated results on Multi-Animate. The samples we tested cover head, half-body, and whole-body scales, all of which produce coherent, realistic, and natural speaker videos. As shown in the bottom row, our method does not require restricting the character’s position; it can appear anywhere in the reference image. These results demonstrate that our proposed VersaAnimator generalizes effectively to diverse characters and body scales.

**Comparisons of Detail Preservation.** As shown in Figure 5, our method effectively preserves the details of the

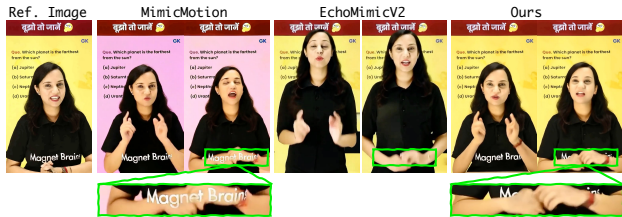


Figure 5. Comparison in pose-driven human animation setting. Focus on the background preservation, hand clarity, the occlusion relationship between the hands and the clothing pattern.

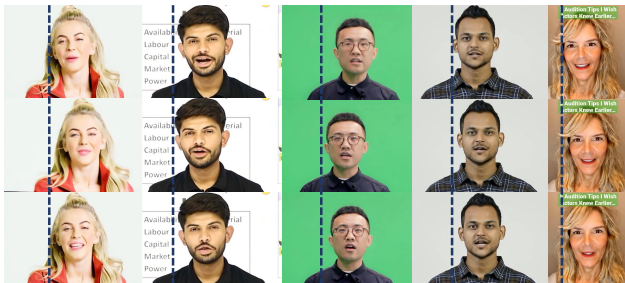


Figure 6. Visual illustration of natural head movement.

reference image, such as the pattern on the clothes (green box), the background, and the character’s position. It is worth noting that when the hand movement would be in front of the pattern of the clothes (green box), the part occluded by hands is not shown, in line with the world law.

**Comparisons with Pose-Driven Body Methods.** Figure 5 also shows that VersaAnimator achieves better clarity in local areas, such as the hands, with additional comparisons provided in the supplementary material.

**Visual Illustration of Natural Head Movement.** The introduction of 3D human motion allows the person to move as a whole, with the head naturally following the body’s movement, aligning with the natural flow of real human speech. As shown in Figure 5, our method enables natural head movement, enhancing the realism and fluidity.

**Visual Illustration of Text Control.** As shown in Figure 8, we present several cases of text prompts to customize the character’s motion in the video. These motions are absent





Figure 7. Qualitative comparison on whether to use code-pose translation module. Left: Stiff and unnatural without pose translation. Right: More natural and fluid motion with pose translation.

from the training videos. This demonstrates that our method can enhance the diversity of generated actions in videos and improve user control over the video generation process.

### 4.3. Qualitative Results

**Multi-scale Talking Body Evaluation.** To evaluate the performance of human video generation, we conduct a comprehensive comparison with the current open-source methods, MimicMotion and EchoMimicV2. Our input also includes the pose for alignment. As shown in Table 1, our VersaAnimator outperforms the state-of-the-art methods across most key metrics, ranking first in quality metrics (FID, FVD, SSIM, and PSNR), synchronization metrics (Sync-C and Sync-D), and the consistency metric (CSIM). \* indicates the version where only audio is used as input, which is more difficult but more valuable. Even in these challenging settings, the purely audio-driven version still performs on par with other methods that use pose prompts. Note that our benchmark includes talking videos with a variety of visible body regions. These results demonstrate VersaAnimator’s robustness and strength.

**Text-to-motion Evaluation.** In order to test the text control capabilities in our pipeline, we keep the audio during evaluation, and we randomly sample audio pieces as input for each test sample. Table 2 presents a comparison of our method with state-of-the-art approaches. Our VersaAnimator outperforms these methods in most key metrics, ranking first in R-Precision (Top-2) and FID, and second in R-Precision (Top-1, Top-3). This demonstrates that, even with audio as an additional input, the motions we generate maintain strong semantic consistency and realism.

### 4.4. Ablation Study

**Analysis of Code-pose Translation Module.** As shown in Table 1, row 5 indicates the impact of our code-pose translation module. It significantly enhances the quality metric (FID, FVD, SSIM, and PSNR). As shown in Figure 7, this module largely alleviates the stiffness and unreality associated with 3D human modeling.

**Analysis of the Fusion Method for Text and Audio Conditions.** To evaluate the multimodal fusion strategy, we replace the per-layer fusion approach with fusion at the last

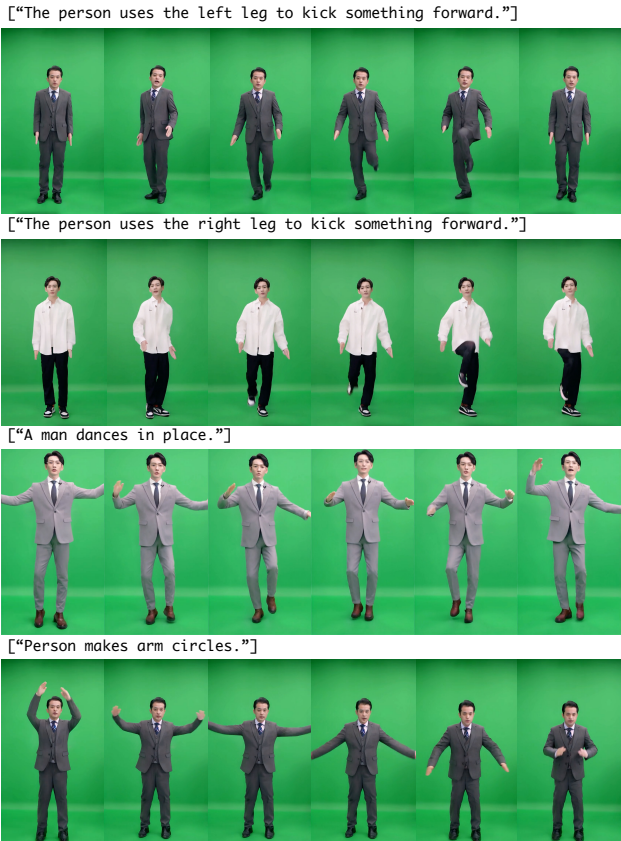


Figure 8. Visual illustration of text control for customizing the character’s motion in the generated video.

layer. As shown in Table 1, row 6 demonstrates that this strategy significantly improves all metrics by progressively fusing audio and text clues at each layer, thereby enhancing the accuracy of the generated output. To verify the impact of the text branch on the original generative capability of the audio, we remove the text branch. As shown in row 7, this fusion strategy allows both modalities to collaborate effectively without audio and text clues.

## 5. Conclusion

In this paper, we highlight the challenges faced in the application of human animation, particularly in supporting diverse scenarios that involve different visible areas of human bodies and enabling fine-grained control of body motion by text prompts. We propose VersaAnimator, a versatile audio-driven human video generation method that synthesizes natural and expressive talking human videos, from head to whole-body animation, which allows users to customize the body motion along with well synchronized lip and facial movements. Our comprehensive experiments demonstrate that VersaAnimator outperforms existing methods, enhancing both user-friendly interaction and the overall experience in human animation.



## Impact Statement

This paper presents work whose goal is to advance the field of Machine Learning, with potential applications in Deepfake generation (Mirsky & Lee, 2021).

## References

- Ahn, H., Ha, T., Choi, Y., Yoo, H., and Oh, S. Text2action: Generative adversarial synthesis from language to action. In *2018 IEEE International Conference on Robotics and Automation (ICRA)*, May 2018. doi: 10.1109/icra.2018.8460608.
- Ahuja, C. and Morency, L.-P. Language2pose: Natural language grounded pose forecasting. In *2019 International Conference on 3D Vision (3DV)*, Sep 2019. doi: 10.1109/3dv.2019.00084.
- Athanasίου, N., Petrovich, M., Black, M., and Varol, G. Teach: Temporal action composition for 3d humans. Sep 2022.
- Cai, Z., Yin, W., Zeng, A., Wei, C., Sun, Q., Yanjun, W., Pang, H. E., Mei, H., Zhang, M., Zhang, L., et al. Smplx: Scaling up expressive human pose and shape estimation. *Advances in Neural Information Processing Systems*, 36, 2024.
- Chang, D., Shi, Y., Gao, Q., Fu, J., Xu, H., Song, G., Yan, Q., Yang, X., and Soleymani, M. Magicedance: Realistic human dance video generation with motions & facial expressions transfer. *CoRR*, 2023.
- Chen, X., Jiang, B., Liu, W., Huang, Z., Fu, B., Chen, T., Yu, J., and Yu, G. Executing your commands via motion diffusion in latent space. Dec 2022.
- Chen, X., Jiang, B., Liu, W., Huang, Z., Fu, B., Chen, T., and Yu, G. Executing your commands via motion diffusion in latent space. In *Proceedings of the IEEE/CVF Conference on Computer Vision and Pattern Recognition*, pp. 18000–18010, 2023.
- Chen, Z., Cao, J., Chen, Z., Li, Y., and Ma, C. Echomimic: Lifelike audio-driven portrait animations through editable landmark conditions. *arXiv preprint arXiv:2407.08136*, 2024.
- Corona, E., Zanfiri, A., Bazavan, E., Kolotouros, N., Alldieck, T., and Sminchisescu, C. Vlogger: Multimodal diffusion for embodied avatar synthesis.
- Dabral, R., Mughal, M., Golyanik, V., and Theobalt, C. Mofusion: A framework for denoising-diffusion-based motion synthesis. Dec 2022.
- Deng, J., Guo, J., and Zafeiriou, S. Arcface: Additive angular margin loss for deep face recognition. 2018.
- Deng, Y., Yang, J., Xu, S., Chen, D., Jia, Y., and Tong, X. Accurate 3d face reconstruction with weakly-supervised learning: From single image to image set. In *Proceedings of the IEEE/CVF conference on computer vision and pattern recognition workshops*, pp. 0–0, 2019.
- Dou, Z., Chen, X., Fan, Q., Komura, T., and Wang, W. C-case: Learning conditional adversarial skill embeddings for physics-based characters. In *SIGGRAPH Asia 2023 Conference Papers*, Dec 2023. doi: 10.1145/3610548.3618205.
- Feng, M., Liu, J., Yu, K., Yao, Y., Hui, Z., Guo, X., Lin, X., Xue, H., Shi, C., Li, X., et al. Dreamoving: A human dance video generation framework based on diffusion models. *arXiv preprint arXiv:2312.05107*, 2023.
- Guo, C., Zou, S., Zuo, X., Wang, S., Ji, W., Li, X., and Cheng, L. Generating diverse and natural 3d human motions from text.
- Guo, C., Zuo, X., Wang, S., Zou, S., Sun, Q., Deng, A., Gong, M., and Cheng, L. Action2motion: Conditioned generation of 3d human motions. In *Proceedings of the 28th ACM International Conference on Multimedia*, Oct 2020a. doi: 10.1145/3394171.3413635.
- Guo, C., Zuo, X., Wang, S., Zou, S., Sun, Q., Deng, A., Gong, M., and Cheng, L. Action2motion: Conditioned generation of 3d human motions. In *Proceedings of the 28th ACM International Conference on Multimedia*, pp. 2021–2029, 2020b.
- Guo, C., Zou, S., Zuo, X., Wang, S., Ji, W., Li, X., and Cheng, L. Generating diverse and natural 3d human motions from text. In *Proceedings of the IEEE/CVF Conference on Computer Vision and Pattern Recognition*, pp. 5152–5161, 2022a.
- Guo, C., Zuo, X., Wang, S., and Cheng, L. Tm2t: Stochastic and tokenized modeling for the reciprocal generation of 3d human motions and texts. In *European Conference on Computer Vision*, pp. 580–597. Springer, 2022b.
- Guo, C., Mu, Y., Javed, M. G., Wang, S., and Cheng, L. Momask: Generative masked modeling of 3d human motions. In *Proceedings of the IEEE/CVF Conference on Computer Vision and Pattern Recognition*, pp. 1900–1910, 2024.
- Heusel, M., Ramsauer, H., Unterthiner, T., Nessler, B., and Hochreiter, S. Gans trained by a two time-scale update rule converge to a local nash equilibrium. *Advances in neural information processing systems*, 30, 2017.
- Hore, A. and Ziou, D. Image quality metrics: Psnr vs. ssim. In *2010 20th international conference on pattern recognition*, pp. 2366–2369. IEEE, 2010.

- Hu, L. Animate anyone: Consistent and controllable image-to-video synthesis for character animation. In *Proceedings of the IEEE/CVF Conference on Computer Vision and Pattern Recognition*, pp. 8153–8163, 2024.
- Karras, J., Holynski, A., Wang, T.-C., and Kemelmacher-Shlizerman, I. Dreampose: Fashion image-to-video synthesis via stable diffusion. In *2023 IEEE/CVF International Conference on Computer Vision (ICCV)*, pp. 22623–22633. IEEE, 2023.
- Langley, P. Crafting papers on machine learning. In Langley, P. (ed.), *Proceedings of the 17th International Conference on Machine Learning (ICML 2000)*, pp. 1207–1216, Stanford, CA, 2000. Morgan Kaufmann.
- Lee, T., Moon, G., and Lee, K. Multiact: Long-term 3d human motion generation from multiple action labels. Dec 2022.
- Li, B., Zhao, Y., Shi, Z., and Sheng, L. Danceformer: Music conditioned 3d dance generation with parametric motion transformer. a.
- Li, F.-L., Zhao, Z., Lu, Q., Lin, X., Chen, H., Chen, B., Pu, L., Zhang, J., Sun, F., Liu, X., et al. Alime avatar: multi-modal content production and presentation for live-streaming e-commerce. In *Proceedings of the 44th International ACM SIGIR Conference on Research and Development in Information Retrieval*, pp. 2635–2636, 2021a.
- Li, R., Zhang, Y., Zhang, Y., Zhang, H., Guo, J., Zhang, Y., Liu, Y., Li, X., Laboratory, P., and Meshcapade, M. Lodge: A coarse to fine diffusion network for long dance generation guided by the characteristic dance primitives. b.
- Li, R., Yang, S., Ross, D. A., and Kanazawa, A. Ai choreographer: Music conditioned 3d dance generation with aist++. In *2021 IEEE/CVF International Conference on Computer Vision (ICCV)*, Oct 2021b. doi: 10.1109/iccv48922.2021.01315.
- Li, T., Zheng, R., Yang, M., Chen, J., and Yang, M. Ditto: Motion-space diffusion for controllable realtime talking head synthesis. *arXiv preprint arXiv:2411.19509*, 2024.
- Lin, G., Jiang, J., Liang, C., Zhong, T., Yang, J., and Zheng, Y. Cyberhost: Taming audio-driven avatar diffusion model with region codebook attention. *arXiv preprint arXiv:2409.01876*, 2024.
- Lin, X. and Amer, M. Human motion modeling using dvgans. *arXiv: Computer Vision and Pattern Recognition, arXiv: Computer Vision and Pattern Recognition*, Apr 2018.
- Loper, M., Mahmood, N., Romero, J., Pons-Moll, G., and Black, M. J. Smpl: A skinned multi-person linear model. In *Seminal Graphics Papers: Pushing the Boundaries, Volume 2*, pp. 851–866. 2023.
- Lu, S., Chen, L.-H., Zeng, A., Lin, J., Zhang, R., Zhang, L., and Shum, H.-Y. Humantomato: Text-aligned whole-body motion generation. Oct 2023.
- Ma, Y., Zhang, S., Wang, J., Wang, X., Zhang, Y., and Deng, Z. Dreamtalk: When expressive talking head generation meets diffusion probabilistic models. *arXiv e-prints*, pp. arXiv–2312, 2023.
- Ma, Y., He, Y., Cun, X., Wang, X., Chen, S., Li, X., and Chen, Q. Follow your pose: Pose-guided text-to-video generation using pose-free videos. In *Proceedings of the AAAI Conference on Artificial Intelligence*, volume 38, pp. 4117–4125, 2024.
- Mahmood, N., Ghorbani, N., Troje, N. F., Pons-Moll, G., and Black, M. J. Amass: Archive of motion capture as surface shapes. In *Proceedings of the IEEE/CVF international conference on computer vision*, pp. 5442–5451, 2019.
- Meng, R., Zhang, X., Li, Y., and Ma, C. Echomimicv2: Towards striking, simplified, and semi-body human animation. *arXiv preprint arXiv:2411.10061*, 2024.
- Mirsky, Y. and Lee, W. The creation and detection of deep-fakes: A survey. *ACM computing surveys (CSUR)*, 54(1): 1–41, 2021.
- Paszke, A., Gross, S., Massa, F., Lerer, A., Bradbury, J., Chanan, G., Killeen, T., Lin, Z., Gimelshein, N., Antiga, L., et al. Pytorch: An imperative style, high-performance deep learning library. 2019.
- Petrovich, M., Black, M. J., and Varol, G. Action-conditioned 3d human motion synthesis with transformer vae. In *2021 IEEE/CVF International Conference on Computer Vision (ICCV)*, Oct 2021. doi: 10.1109/iccv48922.2021.01080.
- Petrovich, M., Black, M., and Varol, G. Temos: Generating diverse human motions from textual descriptions. Apr 2022.
- Prajwal, K., Mukhopadhyay, R., Namboodiri, V. P., and Jawahar, C. A lip sync expert is all you need for speech to lip generation in the wild. In *Proceedings of the 28th ACM international conference on multimedia*, pp. 484–492, 2020.
- Raab, S., Leibovitch, I., Li, P., Aberman, K., Sorkine-Hornung, O., and Cohen-Or, D. Modi: Unconditional motion synthesis from diverse data. Jun 2022.

- Radford, A., Kim, J. W., Hallacy, C., Ramesh, A., Goh, G., Agarwal, S., Sastry, G., Askell, A., Mishkin, P., Clark, J., et al. Learning transferable visual models from natural language supervision. In *International conference on machine learning*, pp. 8748–8763. PMLR, 2021.
- Rombach, R., Blattmann, A., Lorenz, D., Esser, P., and Ommer, B. High-resolution image synthesis with latent diffusion models. In *Proceedings of the IEEE/CVF conference on computer vision and pattern recognition*, pp. 10684–10695, 2022.
- Schneider, S., Baevski, A., Collobert, R., and Auli, M. wav2vec: Unsupervised pre-training for speech recognition. *arXiv preprint arXiv:1904.05862*, 2019.
- Seeger, A.-M., Pfeiffer, J., and Heinzl, A. Texting with humanlike conversational agents: Designing for anthropomorphism. *Journal of the Association for Information systems*, 22(4):8, 2021.
- Seitz, L., Bekmeier-Feuerhahn, S., and Gohil, K. Can we trust a chatbot like a physician? a qualitative study on understanding the emergence of trust toward diagnostic chatbots. *International Journal of Human-Computer Studies*, 165:102848, 2022.
- Shafir, Y., Tevet, G., Kapon, R., and Bermano, A. H. Human motion diffusion as a generative prior. *arXiv preprint arXiv:2303.01418*, 2023.
- Siyao, L., Yu, W., Gu, T., Lin, C., Wang, Q., Qian, C., Loy, C., and Liu, Z. Bailando: 3d dance generation by actor-critic gpt with choreographic memory.
- Tevet, G., Gordon, B., Hertz, A., Bermano, A., and Cohen-Or, D. Motionclip: Exposing human motion generation to clip space.
- Tevet, G., Raab, S., Gordon, B., Shafir, Y., Bermano, A., and Cohen-Or, D. Human motion diffusion model. Sep 2022.
- Tian, L., Wang, Q., Zhang, B., and Bo, L. Emo: Emote portrait alive generating expressive portrait videos with audio2video diffusion model under weak conditions. In *European Conference on Computer Vision*, pp. 244–260. Springer, 2025.
- Tseng, J., Castellon, R., and Liu, C. Edge: Editable dance generation from music. Nov 2022.
- Unterthiner, T., Van Steenkiste, S., Kurach, K., Marinier, R., Michalski, M., and Gelly, S. Towards accurate generative models of video: A new metric & challenges. *arXiv preprint arXiv:1812.01717*, 2018.
- Van Den Oord, A., Vinyals, O., et al. Neural discrete representation learning. volume 30, 2017.
- Wang, C. T2m-hifigpt: Generating high quality human motion from textual descriptions with residual discrete representations. *arXiv preprint arXiv:2312.10628*, 2023.
- Wang, C., Tian, K., Zhang, J., Guan, Y., Luo, F., Shen, F., Jiang, Z., Gu, Q., Han, X., and Yang, W. V-express: Conditional dropout for progressive training of portrait video generation. *arXiv preprint arXiv:2406.02511*, 2024a.
- Wang, T., Li, L., Lin, K., Zhai, Y., Lin, C.-C., Yang, Z., Zhang, H., Liu, Z., and Wang, L. Disco: Disentangled control for realistic human dance generation. In *Proceedings of the IEEE/CVF Conference on Computer Vision and Pattern Recognition*, pp. 9326–9336, 2024b.
- Wang, T.-C., Mallya, A., and Liu, M.-Y. One-shot free-view neural talking-head synthesis for video conferencing. In *Proceedings of the IEEE/CVF conference on computer vision and pattern recognition*, pp. 10039–10049, 2021.
- Wang, Z., Chen, Y., Liu, T., Zhu, Y., Liang, W., and Huang, S. Humanise: Language-conditioned human motion generation in 3d scenes.
- Wang, Z., Bovik, A. C., Sheikh, H. R., and Simoncelli, E. P. Image quality assessment: from error visibility to structural similarity. *IEEE transactions on image processing*, 13(4):600–612, 2004.
- Xu, L., Song, Z., Wang, D., Su, J., Fang, Z., Ding, C., Gan, W., Yan, Y., Jin, X., Yang, X., Zeng, W., and Wu, W. Actformer: A gan-based transformer towards general action-conditioned 3d human motion generation. Mar 2022.
- Xu, M., Li, H., Su, Q., Shang, H., Zhang, L., Liu, C., Wang, J., Yao, Y., and Zhu, S. Hallo: Hierarchical audio-driven visual synthesis for portrait image animation. *arXiv preprint arXiv:2406.08801*, 2024a.
- Xu, S., Chen, G., Guo, Y.-X., Yang, J., Li, C., Zang, Z., Zhang, Y., Tong, X., and Guo, B. Vasa-1: Lifelike audio-driven talking faces generated in real time. *arXiv preprint arXiv:2404.10667*, 2024b.
- Xu, Z., Zhang, J., Liew, J. H., Yan, H., Liu, J.-W., Zhang, C., Feng, J., and Shou, M. Z. Magicanimate: Temporally consistent human image animation using diffusion model. In *Proceedings of the IEEE/CVF Conference on Computer Vision and Pattern Recognition*, pp. 1481–1490, 2024c.
- Yan, S., Li, Z., Xiong, Y., Yan, H., and Lin, D. Convolutional sequence generation for skeleton-based action synthesis. In *2019 IEEE/CVF International Conference on Computer Vision (ICCV)*, Oct 2019. doi: 10.1109/iccv.2019.00449.

- Yang, Z., Zeng, A., Yuan, C., and Li, Y. Effective whole-body pose estimation with two-stages distillation. In *Proceedings of the IEEE/CVF International Conference on Computer Vision*, pp. 4210–4220, 2023.
- Yin, F., Zhang, Y., Cun, X., Cao, M., Fan, Y., Wang, X., Bai, Q., Wu, B., Wang, J., and Yang, Y. Styleheat: One-shot high-resolution editable talking face generation via pre-trained stylegan. In *European conference on computer vision*, pp. 85–101. Springer, 2022.
- Zhang, J., Zhang, Y., Cun, X., Zhang, Y., Zhao, H., Lu, H., Shen, X., and Shan, Y. Generating human motion from textual descriptions with discrete representations. In *Proceedings of the IEEE/CVF conference on computer vision and pattern recognition*, pp. 14730–14740, 2023a.
- Zhang, M., Cai, Z., Pan, L., Hong, F., Guo, X., Yang, L., and Liu, Z. Motiondiffuse: Text-driven human motion generation with diffusion model. Aug 2022a.
- Zhang, M., Cai, Z., Pan, L., Hong, F., Guo, X., Yang, L., and Liu, Z. Motiondiffuse: Text-driven human motion generation with diffusion model. *arXiv preprint arXiv:2208.15001*, 2022b.
- Zhang, M., Guo, X., Pan, L., Cai, Z., Hong, F., Li, H., Yang, L., and Liu, Z. Remodiffuse: Retrieval-augmented motion diffusion model. In *Proceedings of the IEEE/CVF International Conference on Computer Vision*, pp. 364–373, 2023b.
- Zhang, M., Li, H., Cai, Z., Ren, J., Yang, L., and Liu, Z. Finemogen: Fine-grained spatio-temporal motion generation and editing. *Advances in Neural Information Processing Systems*, 36, 2024a.
- Zhang, W., Cun, X., Wang, X., Zhang, Y., Shen, X., Guo, Y., Shan, Y., and Wang, F. Sadtalker: Learning realistic 3d motion coefficients for stylized audio-driven single image talking face animation. In *Proceedings of the IEEE/CVF Conference on Computer Vision and Pattern Recognition*, pp. 8652–8661, 2023c.
- Zhang, Y., Black, M., and Tang, S. Perpetual motion: Generating unbounded human motion. *arXiv: Computer Vision and Pattern Recognition, arXiv: Computer Vision and Pattern Recognition*, Jul 2020.
- Zhang, Y., Gu, J., Wang, L.-W., Wang, H., Cheng, J., Zhu, Y., and Zou, F. Mimicmotion: High-quality human motion video generation with confidence-aware pose guidance. *arXiv preprint arXiv:2406.19680*, 2024b.
- Zhao, R., Su, H., and Ji, Q. Bayesian adversarial human motion synthesis. In *2020 IEEE/CVF Conference on Computer Vision and Pattern Recognition (CVPR)*, Jun 2020. doi: 10.1109/cvpr42600.2020.00626.
- Zhou, Y., Barnes, C., Lu, J., Yang, J., and Li, H. On the continuity of rotation representations in neural networks. In *Proceedings of the IEEE/CVF conference on computer vision and pattern recognition*, pp. 5745–5753, 2019.
- Zhu, S., Chen, J. L., Dai, Z., Dong, Z., Xu, Y., Cao, X., Yao, Y., Zhu, H., and Zhu, S. Champ: Controllable and consistent human image animation with 3d parametric guidance. In *European Conference on Computer Vision*, pp. 145–162. Springer, 2025.



## A. Implementation Details.

For text-controlled, audio-driven motion generation, we set the codebook as  $512 \times 512$ , *i.e.*, 512 512-dimension dictionary vectors. Following (Guo et al., 2024; Zhang et al., 2023a), the dataset HumanML3D is extracted into motion features with dimensions 263, which related to local joints position, velocity, and rotations in root space as well as global translation and rotations. The joint number is set to 22. The transformer is composed of 8 transformer layers, with 6 heads and a latent dimension of 384.

We train our diffusion model on 40 hours of self-recorded and web-collected news broadcast videos with synchronized audio and visual content. The dataset is balanced across diverse ethnicities, languages, and shot scales. The average length of the training video clips is 10 seconds. The video diffusion module is trained on 8 NVIDIA A100 GPUs (80GB). The first stage, pose2vid, is trained for 10,000 steps, building upon pre-trained weights from Mimicmotion (Zhang et al., 2024b). The second stage, which incorporates audio input, is trained for an additional 36,000 steps.

## B. Comparisons with Pose-driven Body Animation Methods.



Figure 9. Comparisons with pose-driven body animation methods.

We present more comparisons results with pose-driven body animation methods. The visual results in Figure 9 and Figure 10



Figure 10. Comparisons with pose-driven body animation methods.

demonstrate that VersaAnimator maintains superior structural integrity and identity consistency in local regions, such as the hands and face, when compared to the current state-of-the-art methods.

### C. Details of Audio Token.

To enhance the encoding of audio for motion-driven animation, we utilized wav2vec (Schneider et al., 2019) as our audio feature encoder. Specifically, we concatenated the audio embeddings from the final 12 layers of the wav2vec model to capture a richer and more diverse range of semantic information across different audio layers. Considering the sequential nature of audio data and its contextual dependencies, we designed a temporal block to extract and fuse the temporal information. Through multiple convolution layers, we transformed the pre-trained audio embeddings into  $\{c_{\text{audio}}^t\}_{t=1}^{T/l}$ , where  $c_{\text{audio}}^t \in \mathbb{R}^{D_a}$  represents the  $t$ -th audio token. Here,  $l$  is the downsampling rate of the temporal block and  $D_a$  denotes the dimension of the audio token.

## D. Comparison of Motion Amplitude.

We observe that the motion generated by other methods exhibits a limited magnitude around the gesture in the reference image. We download several videos from the official VLOGGER website and test our method for comparison. We extract the dwpose frame by frame from the generated video and visualize the dwpose of the upper limbs. The dwpose of all the frames is superimposed on a single image, representing the entire video. As shown in Figure 11, our method covers a larger active area and is more expressive.

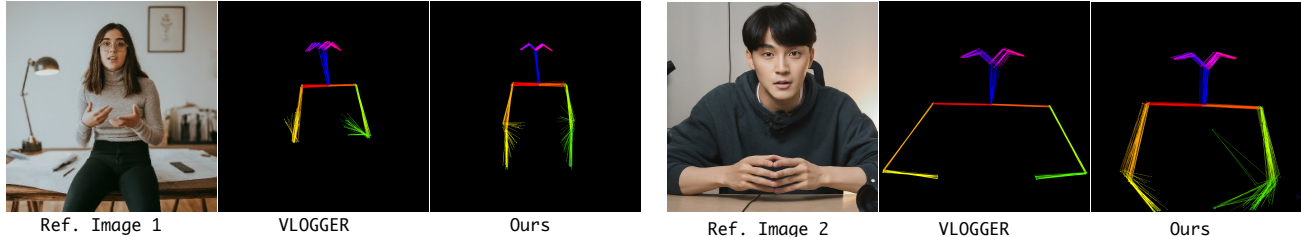


Figure 11. Comparison of motion amplitude with VLOGGER (Corona et al.). We extract the dwpose frame by frame from the generated video and visualize the dwpose of the upper limbs. The dwpose of all the frames is superimposed on a single image, representing the entire video. It can be seen that our method covers a larger active area and is more expressive.

## E. Elaborate Version of Related works.

**Human Motion Generation.** Human motion generation can be broadly categorized into two primary approaches based on the type of input: 1) motion synthesis without conditions (Raab et al., 2022; Tevet et al., 2022; Zhang et al., 2020; Zhao et al., 2020; Yan et al., 2019) and 2) motion synthesis with specified multimodal conditions, such as action labels (Xu et al., 2022; Guo et al., 2020a; Petrovich et al., 2021; Lee et al., 2022; Dou et al., 2023), textual descriptions (Wang et al.; Chen et al., 2022; Lin & Amer, 2018; Ahn et al., 2018; Tevet et al.; Zhang et al., 2022a; Tevet et al., 2022; Petrovich et al., 2022; Athanasiou et al., 2022; Lu et al., 2023; Guo et al.; Ahuja & Morency, 2019), or audio and music (Li et al., b; Tseng et al., 2022; Li et al., a; Dabral et al., 2022; Li et al., 2021b; Siyao et al.). Due to its user-friendly nature and the convenience of language input, text-to-motion is one of the most important motion generation tasks. Given the remarkable success of diffusion-based generative models in other domains (Rombach et al., 2022), some approaches have employed conditional diffusion models for human motion generation (Zhang et al., 2022b; 2023b; 2024a; Chen et al., 2023). Other works (Zhang et al., 2023a; Guo et al., 2024; Wang, 2023) first discretize motions into tokens using vector quantization (Van Den Oord et al., 2017) and then predict the code sequence of motion.

## F. Metric Details and Further Results on Text-to-motion Generation.

Table 3. Evaluation of text-to-motion capability on the HumanML3D test set, with comparison to state-of-the-art methods such as TM2T (Guo et al., 2022b), T2M (Guo et al.), MDM (Shafir et al., 2023), MLD (Chen et al., 2023), MotionDiffuse (Zhang et al., 2022b), T2M-GPT (Zhang et al., 2023a), and ReMoDiffuse (Zhang et al., 2023b).

| METHODS       | R PRECISION $\uparrow$  |                         |                         | FID $\downarrow$        | MULTIMODALIT $\uparrow$ | MULTIMODAL DIST $\downarrow$ |
|---------------|-------------------------|-------------------------|-------------------------|-------------------------|-------------------------|------------------------------|
|               | TOP 1                   | TOP 2                   | TOP 3                   |                         |                         |                              |
| TM2T          | 0.424 $\pm$ .003        | 0.618 $\pm$ .003        | 0.729 $\pm$ .002        | 1.501 $\pm$ .017        | 2.424 $\pm$ .093        | 3.467 $\pm$ .011             |
| T2M           | 0.455 $\pm$ .003        | 0.636 $\pm$ .003        | 0.736 $\pm$ .002        | 1.087 $\pm$ .021        | 2.219 $\pm$ .074        | 3.347 $\pm$ .008             |
| MDM           | -                       | -                       | 0.611 $\pm$ .007        | 0.544 $\pm$ .044        | <b>2.799</b> $\pm$ .072 | 5.566 $\pm$ .027             |
| MLD           | 0.481 $\pm$ .003        | 0.673 $\pm$ .003        | 0.772 $\pm$ .002        | 0.473 $\pm$ .013        | 2.413 $\pm$ .079        | 3.196 $\pm$ .010             |
| MOTIONDIFFUSE | 0.491 $\pm$ .001        | 0.681 $\pm$ .001        | 0.782 $\pm$ .001        | 0.630 $\pm$ .001        | 1.553 $\pm$ .042        | 3.113 $\pm$ .001             |
| T2M-GPT       | 0.492 $\pm$ .003        | 0.679 $\pm$ .002        | 0.775 $\pm$ .002        | 0.141 $\pm$ .005        | 1.831 $\pm$ .048        | 3.121 $\pm$ .009             |
| REMODIFFUSE   | <b>0.510</b> $\pm$ .005 | <b>0.698</b> $\pm$ .006 | <b>0.795</b> $\pm$ .004 | <b>0.103</b> $\pm$ .004 | 1.795 $\pm$ .043        | <b>2.974</b> $\pm$ .006      |
| OURS          | <b>0.505</b> $\pm$ .002 | <b>0.698</b> $\pm$ .003 | <b>0.794</b> $\pm$ .002 | <b>0.090</b> $\pm$ .003 | <b>2.563</b> $\pm$ .071 | <b>2.981</b> $\pm$ .007      |

**Metric details** For motion generation, we follow the common metrics of prior works (Guo et al.) to evaluate the text-



to-motion generation performance. Global representations of motion and text descriptions are first extracted with the pre-trained network in (Guo et al.), and then measured by the following five metrics:

- R-Precision. Given one motion sequence and 32 text descriptions (1 ground-truth and 31 randomly selected mismatched descriptions), we rank the Euclidean distances between the motion and text embeddings. Top-1, Top-2, and Top-3 accuracy of motion-to-text retrieval are reported.
- Frechet Inception Distance (FID). We calculate the distribution distance between the generated and real motion using FID (Heusel et al., 2017) on the extracted motion features.
- Multimodal Distance (MM-Dist). The average Euclidean distances between each text feature and the generated motion feature from this text.
- Multimodality (MModality). For one text description, we generate 30 motion sequences forming 10 pairs of motion. We extract motion features and compute the average Euclidean distances of the pairs. We finally report the average over all the text descriptions.

We present more metrics for comparison with other methods in Table 3. In addition to the metrics discussed in the main text, we rank second in MM-Dist and MModality, respectively. This demonstrates great generative diversity and multimodal alignment capabilities.

## G. Introduction of HumanML3D.

HumanML3D (Guo et al.) is currently the largest 3D human motion dataset with textual descriptions. The dataset contains 14,616 human motions and 44,970 text descriptions. The entire textual descriptions are composed of 5,371 distinct words. The motion sequences are originally from AMASS (Mahmood et al., 2019) and HumanAct12 (Guo et al., 2020b) but with specific pre-processing: motion is scaled to 20 FPS; those that are longer than 10 seconds are randomly cropped to 10-second ones; they are then re-targeted to a default human skeletal template and properly rotated to face Z+ direction initially. Each motion is paired with at least 3 precise textual descriptions. The average length of descriptions is approximately 12. According to (Guo et al.), the dataset is split into training, validation, and test sets with proportions of 80%, 5%, and 15%, respectively. We select the best FID model on the validation set and report its performance on the test set.